Atomic layer deposition of TiO_2-nanomembrane-based photocatalysts with enhanced performance

Riyanto Edy, Gaoshan Huang, Yuting Zhao, Jing Zhang, Yongfeng Mei, and Jianjun Shi

Citation: AIP Advances **6**, 115113 (2016); doi: 10.1063/1.4967783
View online: https://doi.org/10.1063/1.4967783
View Table of Contents: http://aip.scitation.org/toc/adv/6/11
Published by the American Institute of Physics

AIP ADVANCES **6**, 115113 (2016)

Atomic layer deposition of TiO_2-nanomembrane-based photocatalysts with enhanced performance

Riyanto Edy,[1,2] Gaoshan Huang,[2,a] Yuting Zhao,[2] Jing Zhang,[3]
Yongfeng Mei,[2] and Jianjun Shi[3,b]
[1]*State Key Laboratory for Modification of Chemical Fibers and Polymer Materials, College of Material Science and Engineering, Donghua University, Shanghai 201620, People's Republic of China*
[2]*Department of Materials Science, Fudan University, Shanghai 200433, People's Republic of China*
[3]*College of Science, Donghua University, Shanghai 201620, People's Republic of China*

(Received 14 September 2016; accepted 1 November 2016; published online 8 November 2016)

In this study, TiO_2 and TiO_2-ZnO nanomembranes were fabricated by atomic layer deposition using the three-dimensionally porous template and their photocatalytic properties were investigated. The nanomembranes were firstly deposited onto the surface of polyurethane porous sponge templates (sacrificial templates), followed by a calcination at 500 or 800 °C. Three-dimensionally porous structures as a replica of the porous sponge templates were thus achieved. By a pulverizing process, the porous structures were broken into small pieces, which were then employed as photocatalyst. Experimental results show that the degree of crystallinity is raised by increasing of the nanomembrane thickness due to the increase of the grain size with minimizing the number of grain boundaries in the thicker nanomembrane, which is beneficial to enhance the photocatalysis efficiency. On the other hand, the photocatalytic activity can also be improved by TiO_2-ZnO composite, due to lower electron-hole recombination possibility and better carrier conductivity. © *2016 Author(s). All article content, except where otherwise noted, is licensed under a Creative Commons Attribution (CC BY) license (http://creativecommons.org/licenses/by/4.0/).* [http://dx.doi.org/10.1063/1.4967783]

I. INTRODUCTION

Semiconductor nanostructures are becoming an intensive research interest due to improved properties and promising technological applications.[1–6] Especially, oxides semiconductor such as titanium dioxide (TiO_2), zinc oxide (ZnO) and related structures have attracted attention for applications in photocatalysis, gas sensing, and photovoltaic cells.[7–12] The enhancement of photocatalytic properties of the TiO_2-ZnO composite structure, in comparison with TiO_2 oxide has been reported.[8,9,13] It is believed that the coupling of anatase and rutile TiO_2 with ZnO can achieve a more efficient electron-hole pair separation under illumination and, consequently, a higher reaction rate.[14,15] Specifically, the electronic properties modification of the composite materials is invoked to explain this behavior: the electron transfer from the conduction band of ZnO to the conduction band of TiO_2 under illumination and, conversely, the hole transfer from the valence band of TiO_2 to the valence band of ZnO give rise to a decrease of the pairs recombination rate, i.e., to an increase of their lifetime.[13,15] This phenomenon increases the availability of the pairs on the surface of the photocatalyst and an improvement of the occurence of redox processes can be expected.[15]

In this study, TiO_2 and TiO_2-ZnO were deposited by atomic layer deposition (ALD) onto the polyurethane sponge template, which then followed by calcination to form three-dimensionally

---

[a] Gaoshan Huang, Electronic mail: gshuang@fudan.edu.cn
[b] Jianjun Shi, Electronic mail: JShi@dhu.edu.cn

porous structures consisting oxide semiconductor nanomembranes. After a pulverizing process, the formed nanomembranes were employed as photocatalyst with methyl orange (MO) solution as a typical pollutant. The experimental results indicate that the composite structure and the increased thickness have positive effects on the enhanced photocatalytic performance.

II. EXPERIMENTAL

Three-dimensionally porous TiO_2 and TiO_2-ZnO (TZO) composite were produced by ALD on polyurethane sponges (sacrificial templates). During ALD, Tetrakis (dimethylamido) titanium (TDMAT) was employed as Ti source and Diethyl zinc (DEZ) was used as Zn source, with both using water (H_2O) as reactant. Both TDMAT and H_2O were exposed into the ALD chamber with pulse and purge times of 150 ms and 50 s, respectively. Those pulse and purge times were also applied in ZnO deposition. To give more chance of the precursors to travel and reach to all of the porous surfaces, the exit valve of ALD chamber was closed for 2 s at each pulsing step. The ALD chamber temperature was set at 150 °C and the temperatures of TDMAT, DEZ, and H_2O were 105, 45, and 50 °C, respectively. ALD of 50 up to 1000 cycles were used in present work to investigate the influence of the thickness. After deposition, the samples were calcined with temperatures of 500 to 800 °C in the flows of oxygen to remove the sponge template. This technique allows us to obtain pure catalytic materials because the organic materials of the sponge was carbonized at high temperature and react with oxygen to form CO_2.

The thicknesses and morphologies of the samples were imaged by scanning electron microscopy, and the detailed microstructure of the sample is analysed by transmission electron microscopy (TEM, Tecnai F30). The crystal structures of the samples were evaluated by X-ray diffraction (XRD) spectroscopy on a D8 spectrometer of Advance Bruker AXS GMBH, using CuK α radiation with irradiations condition of 40 kV and 40 mA.

The photocatalytic performance of samples was evaluated by photodegradation of MO solution measured by UV-Vis spectrophotometer (Shimadzu UV-2550 spectrometer). The photocatalyst with the weight of 0.0125 g was placed in 50 mL MO solution with an initial concentration of 10 mg/L was kept in the dark for 30 min to achieve the adsorption equilibrium, which then illuminated under the UV light irradiation of 200-W xenon lamp (Lanpu, China) with a distance of 50 cm. The degradation of the MO was measured every 20 min. The absorption intensity at the wavelength of 464 nm is found to be the maximum absorption peak of MO,[16] and the peak intensity was extracted to calculate the MO degradation.

III. RESULTS AND DISCUSSION

Fig. 1 is the schematic of the fabrication process, taking the fabrication of TiO_2 nanomembranes as an example. The original polyurethane sponge template was shown in Fig. 1(a), which then deposited by ALD with coatings of 50 up to 1000 ALD cycles. Polyurethane is a polymer which has functional groups of C=O on the surface that are beneficial to facilitate the initial growth of ALD. Fig. 1(b) shows the SEM image of the sponge deposited with TiO_2 (1000 ALD cycles). It is evident that TiO_2 ALD can be grown uniformly on the surface of porous sponge structure. With porous substrate thickness of 3 mm, the TiO_2 can be deposited easily on all over the surface including the bottom side of the porous sponge. In order to obtain pure photocatalyst for catalysis applications, the deposited sponge was calcined in oxygen atmosphere (Fig. 1(c)). Oxygen reacts to a carbonized sponge material to form CO_2 and flow out from a calcination chamber, which eventually causes the formation of three-dimensionally porous structures consisting of nanomembranes. Fig. 1(d) shows the powder/nanomembranes resulted from the porous TiO_2 structure after calcination and pulverization. In the following photocatalytic applications, nanomembranes formed from the ruined porous TiO_2 structure by pulverizing were employed as photocatalyst.

Cross-sectional images of the TiO_2 nanomembrane fabricated by 200, 400, and 1000 ALD cycles are presented in Figs. 2(a), 2(b), and 2(c), respectively. The SEM images show that the thicknesses increase with ALD cycles: the thicknesses are 28.61, 44.54, and 75.47 nm approximately for samples made by 200, 400, and 1000 ALD cycles, respectively. The fluctuation of the thickness per cycle may

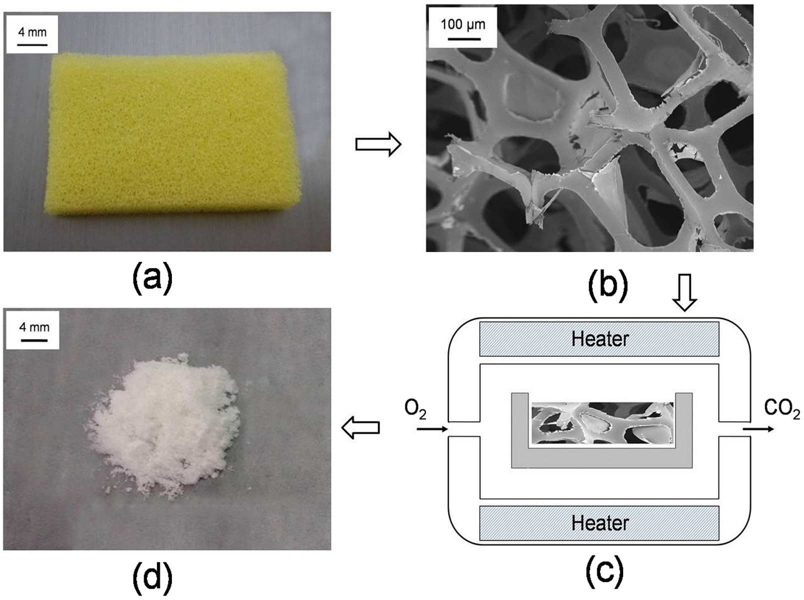

FIG. 1. Schematic of the fabrication process. (a) Photo of polyurethane porous sponge. (b) SEM image of TiO_2 deposited sponge (1000 ALD cycles) before calcination. (c) Calcination process. (d) Photo of the formed TiO_2 nanomembrane achieved after calcination and following manual pulverizing.

be due to the influence from the calcination process since the structures evolutions in nanomembranes with different thicknesses are also different as we will discuss later. On the other hand, the cross-sectional image of TZO composite nanomembrane formed with ALD of TiO_2 (10)/ZnO(10), 11 loops has a thickness of ~ 29.06 nm as shown in Fig. 2(d).

Fig. 3 shows SEM images of TiO_2 nanomembrane formed by 50 to 1000 ALD cycles (Figs. 3(a)–3(c)) and SEM images of TZO composite nanomembrane formed with (d) TiO_2 (10)/ZnO(1), 20 loops, (e) TiO_2(10)/ZnO(5), 15 loops, (f) TiO_2 (10)/ZnO(10), 11 loops, as well as TEM image of TiO_2 nanomembrane formed with 400 ALD cycles and calcined at 500 °C for 3 h

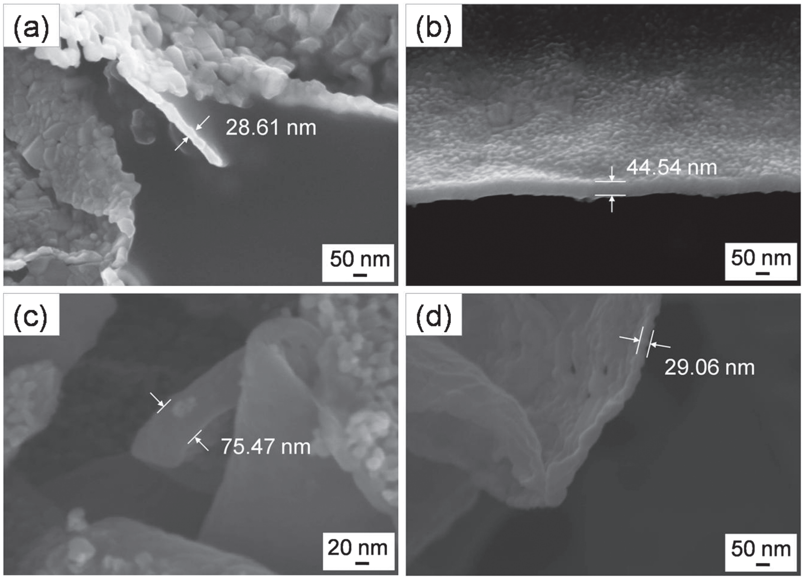

FIG. 2. Cross-sectional SEM images of TiO_2 nanomembrane fabricated by (a) 200, (b) 400, and (c) 1000 ALD cycles. (d) Cross-sectional SEM image of TZO composite nanomembrane formed with ALD of TiO_2 (10)/ZnO(10), 11 loops.

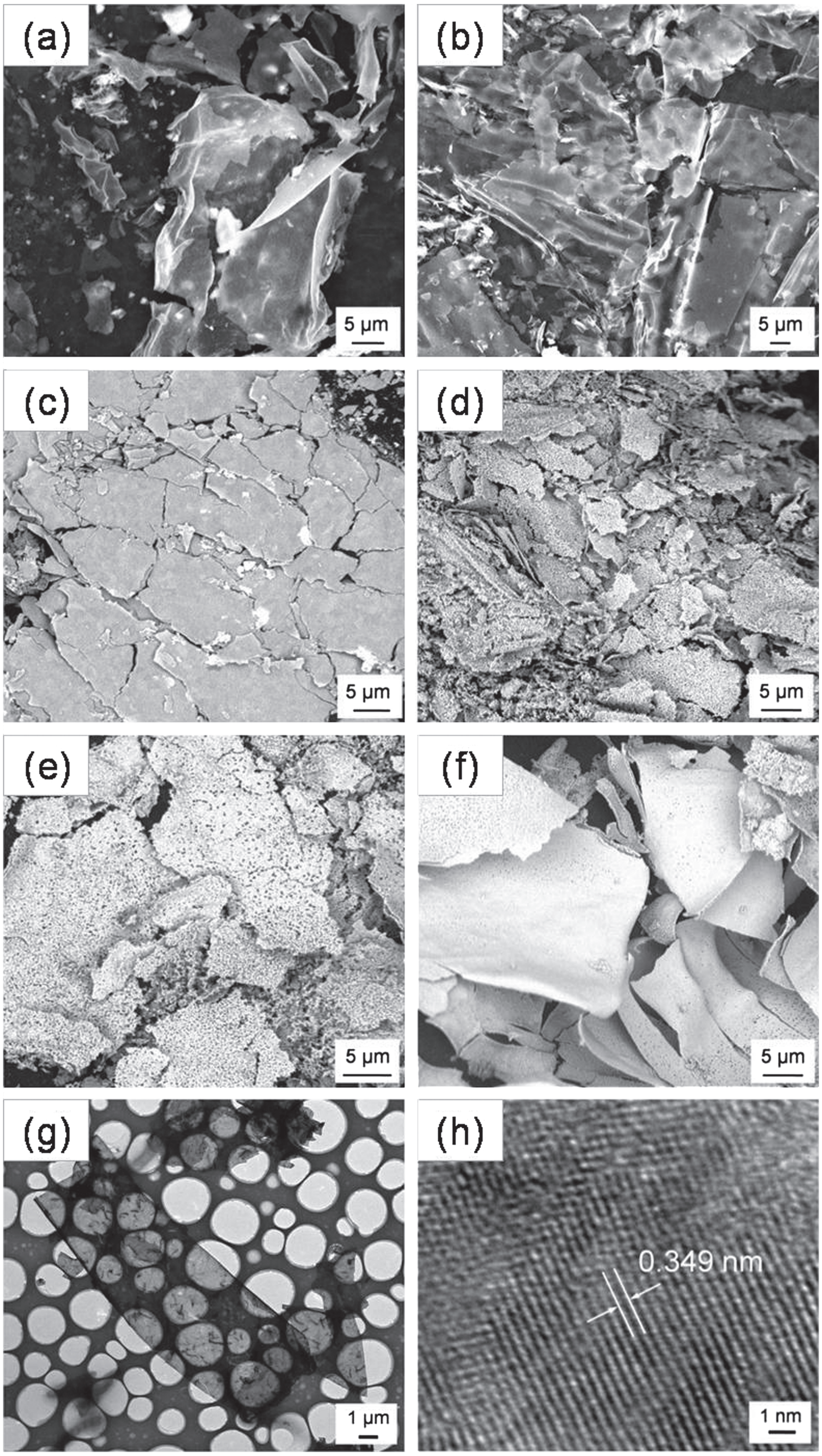

FIG. 3. SEM images of TiO_2 nanomembrane fabricated by (a) 50, (b) 200, and (c) 1000 ALD cycles. SEM images of TZO composite nanomembrane formed with ALD of (d) TiO_2 (10)/ZnO(1), 20 loops, (e) TiO_2 (10)/ZnO(5), 15 loops, and (f) TiO_2 (10)/ZnO(10), 11 loops. (g) TEM image of TiO_2 nanomembrane formed with 400 ALD cycles and calcined at 500 °C for 3 h. (h) Corresponding HRTEM image.

(Fig. 3(g)). One can see that all the TiO_2 and TZO samples consist a large amount of nanomembranes. TiO_2 samples with sheets feature formed with fewer ALD cycles (i.e., thinner nanomembranes) lead to formation of wrinkles and rolled edges (Figs. 3(a)–3(b)). Conversely, the thicker nanomembranes formed with more ALD cycles is achieved nanomembranes with stiffer feature as indicated by plane sheets image without wrinkle and rolled feature (Fig. 3(c)). In addition, the TZO composites in Figs. 3(d)–3(f) demonstrate nanomembranes with similar morphologies, indicating the current approach is capable of mass-producing nanomembranes with different materials. The HRTEM image in Fig. 3(h) show lattice fringe of the calcined TiO_2 nanomembrane where a lattice spacing of 0.349 nm indicates the presence of $\{101\}$ facet of the anatase TiO_2.[17–20] These nanomembranes with thicknesses in the range of tens have an advantage to improve the surface contact area between photocatalyst and solution, which consequently lead to enhancement of the photocatalytic performance, as we will discuss in details later.

Fig. 4(a) show the XRD spectra of TiO_2 samples fabricated with 50, 200, and 400 ALD cycles on the polyurethane sponge templates and calcined at 500 °C (spectra 1-3 in Fig. 4(a)), and 400 and 1000 ALD cycles calcined at 800 °C (spectra 4-5 in Fig. 4(a)), with both calcination time of 3h. The formed crystalline phase of the TiO_2 with various ALD cycles are anatase which has a prominent diffraction peak of (101) facet. It has an agreement to the TEM evaluation of sample formed with 400 ALD cycles and calcined at 500 °C for 3 h (Fig. 3(h)). One can see that the intensity of (101) peak increases with increasing of the ALD cycles and/or raising the calcination temperature (Fig. 4(a)). The increase of the XRD peak intensity indicates the presence of anatase TiO_2 with better crystallinity,[21–24] which are beneficial to the photocatalysis performance, as will be discussed later. Fig. 4(b) shows the XRD patterns of the TZO composite (TiO_2(10)/ZnO(1), 20 loops) calcined at 800 °C for 3h. The presence of wurtzite-type hexagonal phase ZnO is clearly shown in the sample with a strongest diffraction peak of (101) facet of wurtzite structure at 36.25°. Other peaks at 2θ of 31.74, 34.39, 47.51, 56.57, 62.84, 66.33, and 67.89° correspond to (100), (002), (102), (110), (103), (112), and (201) facets of wurtzite structure of ZnO, respectively. In the composite, the apparent peaks of TiO_2 crystalline are also emerges with low intensities at 35.06, 39.31, and 62.88°, indicating the formation of the composite consisting both TiO_2 and ZnO.

Figs. 5(a) and 5(b) show the improvement of photocatalytic performance of TiO_2 samples calcined at 500 and 800 °C as photocatalysts, respectively. It has been well-recognized that the degree of crystallinity is an important factor influencing the photocatalytic activity of TiO_2.[22,25–27] TiO_2 crystallinity will increase with increasing grain size due to the decreasing of the grain boundaries as defect states.[22] The defects can act as trap sites for the photogenerated charge carriers, increasing their probability of recombination.[22,28] Therefore, TiO_2 with fewer defect leads to increasing lifetime of charge carriers, and consequently more separated electrons and holes can migrate to the photocatalyst surface that are beneficial for reduction and oxidation processes in the decomposition of MO.[4,19,29–31] In our previous study,[32] although it cannot be observed directly in XRD, the as-prepared (without calcination) TiO_2 with fewer ALD cycles has a lower degree of local order, on the contrary more ALD cycles leading to an improvement of the degree of local order. This phenomenon has also been noticed in previous studies carried out by Alekhin *et al.*[33] and Moret *et al.*[34] In the

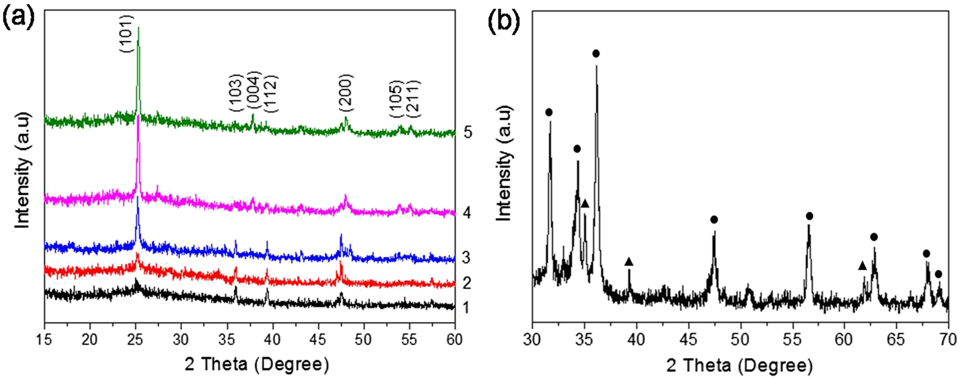

FIG. 4. (a) XRD spectra of TiO_2 samples formed with (1) 50, (2) 200, (3) 400 ALD cycles calcined at 500 °C, and (4) 400, (5) 1000 ALD cycles calcined at 800 °C, (JCPDS Card No.21-1272). (b) XRD spectrum of TiO_2-ZnO composite (TiO_2(10)/ZnO(1), 20 loops) calcined at 800 °C (● and ▲ denote wurtzite structure of ZnO and TiO_2 crystalline, respectively).

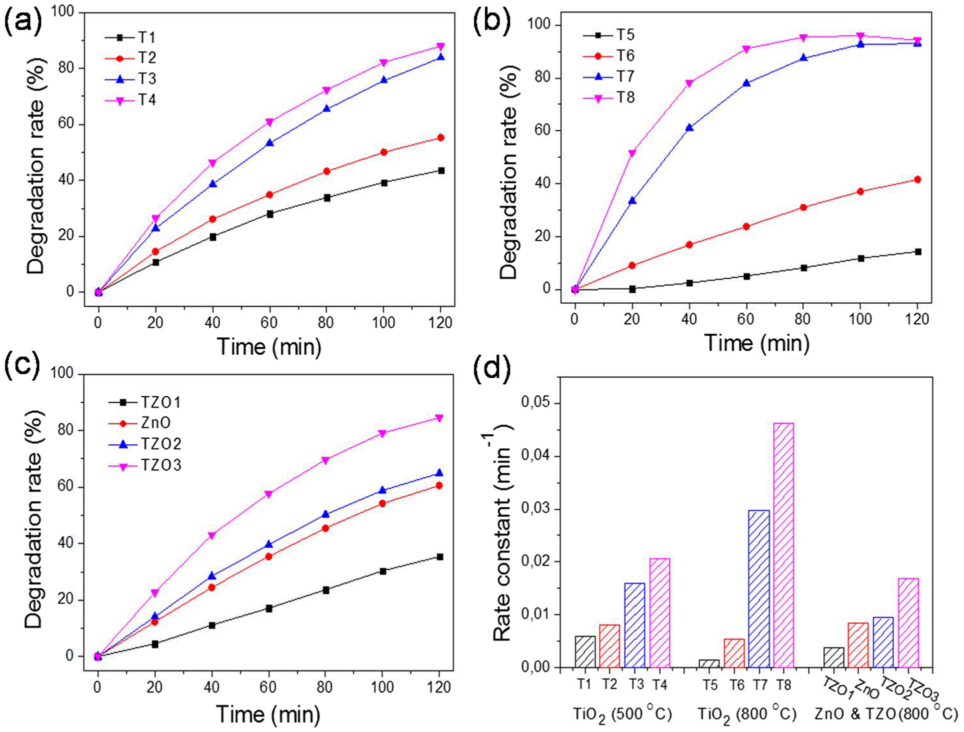

FIG. 5. Photocatalytic performance of TiO_2 photocatalyst formed with (a) (T1) 50, (T2) 200, (T3) 400, and (T4) 1000 ALD cycles calcined at 500 °C and (b) (T5) 50, (T6) 200, (T7) 400, and (T8) 1000 ALD cycles calcined at 800 °C. (c) Photocatalytic performance of ZnO (200 cycles) and TZO composite formed with (TZO1) TiO_2 (10)/ZnO(1), 20 loops, (TZO2) TiO_2 (10)/ZnO(5), 15 loops, and (TZO3) TiO_2 (10)/ZnO(10), 11 loops, calcined at 800 °C. (d) Rate constant of TiO_2, ZnO, and TZO composites.

transformation from amorphous tocrystalline by calcination, the TiO_2 with lower degree of local order leds to be transformed into crystallized TiO_2 with lower degree of crystallinity and conversely, the TiO_2 amorphous with higher degree of local order is able to be transformed into TiO_2 crystalline with higher degree of crystallinity as indicated by the intensity of (101) peak in XRD (Fig. 4(a)). The degree of crystallization improves with increasing grain size as the influence of the grain boundaries decrease.[22] In addition, in the crystalline growth during calcination, the increase of nanomembrane thickness leading to an enhancement of the grain size due to a vertical growth. As a result, the degree of crystallization and the catalytic activity increases by raising the TiO_2 thickness (from 50 to 1000 ALD cycles, Figs. 5(a) and 5(b)). On the other hand, the increase of calcination temperature from 500 to 800 °C of the samples with higher degree of local order (400 and 1000 ALD cycles) has effect to gain anatase phase with improved crystalinity (Fig. 4(a)) and thus has a substantial contribution to the enhanced photocatalytic activity (Fig. 5(b)).[23,26,35] It was indicated by the photocatalytic test that the MO solution can be degraded totally with the photocatalysts formed by 400 and 1000 ALD cycles (Fig. 5(b)), and the performance of samples calcinated at 800 °C is obviously better than that of the photocatalyst calcined at 500 °C (Figs. 5(a) and 5(b)).

Previously, it is noticed that composite semiconductor structures can effectively decrease the electron-hole recombination and therefore lead to enhanced photocatalytic performance.[9,36,37] Fig. 5(c) shows the photocatalytic performance of ZnO with 200 ALD cycles and the TZO composites synthesized by ALD with calcination temperature of 800 °C. It revealed that the photocatalytic performance of ZnO is better than TiO_2 for the same deposition of 200 ALD cycles (Figs. 5(b) and 5(c)), which are attributed to the ability of ZnO to generate H_2O_2 more efficiently than TiO_2 as well as more active sites with high surface reactivity.[23,38–40] On the other hand, the photocatalytic activity of TZO composite with thickness ratios of 5:10 and 10:10 structure are increased significantly compared to the photocatalytic performance of TiO_2 and ZnO with 200 ALD cycles although the samples were all annealed at 800 °C (Figs. 5(b) and 5(c)). In present case, we consider that the enhancement of the photocatalytic performance is due to the band gap coupling among the different materials in the composite leading to a better charge separation and transportation, which in turn increases the lifetime of charge carriers by reducing their recombination-rate.[8,9,41] Correspondingly, the diffusion length of electrons and holes to reach the interface oxide-organic material is increased.[8] Additional factor that can contribute to the increase of photocatalytic activity is the presence of a high electric conductive phases of ZnO with a better conductivity property, which leads to an increase of the probability of the carriers reaching the photocatalyst/solution interface.[8]

In addition, the evolution of photocatalytic activities of the TZO composites with different ZnO concentrations (TZO1: TiO_2 (10)/ZnO(1), 20 loops, TZO2: TiO_2 (10)/ZnO(5), 15 loops, and TZO3: TiO_2 (10)/ZnO(10), 11 loops) is exhibited in Fig. 5(c). Promoted photocatalytic performance (except TZO1) and enhanced photocatalytic performance with increasing the ZnO concentration can be noticed. As a conductive material, ZnO in the hexagonal wurtzite structure can be obtained in the as-deposited ALD films even when using relatively low deposition temperature.[44,45] Generally, the crystallinity should be raised by increasing the thickness, and a higher crystallinity is followed by a higher conductivity,[34] which suggests that a single ZnO ALD layer can not be well transformed by calcination into a crystal structure with high conductivity. In our experiment, the presence of ZnO monolayer inserted in TZO composite can not effectively be functionalized as a conductive layer, and as a result, the sample TZO1 has a relatively lower photocatalytic performance.

Generally, the photocatalytic degradation of the MO follows a pseudo-first-order reaction with its kinetics can be expressed as $\ln (C_0/C) = k \cdot t$, where t is the irradiation time, C_0 and C represent the initial and reaction concentrations, respectively.[46–48] Then, the pseudo first-order constant k in the degradation process can be calculated to evaluate the photocatalytic efficiency. Fig. 5(d) summarizes the rate constants of TiO_2, ZnO (200 cycles), and TZO samples. The TiO_2 photocatalyst formed by ALD with 1000 cycles calcined at 800 °C demonstrates the highest degradation efficiency and MO can be degraded totally for UV-light illumination of 100 min, which corresponds to the pseudo first-order rate constant of 0.0463 min^{-1}. When compare the photocatalytic performance of TZO composite and pure TiO_2, one may notice that the performance of TZO1 is even worse than that of T1. We ascribe this to the poor crystalinity in TZO1 due to the insertion of ZnO layer in the sample, which may disturb the crystallization of TiO_2 during annealing. However, with further increase of ZnO concentration (TZO2 and TZO3), the aforementioned band gap coupling effect and the good conductivity gradually play important role, and overcome the side effect from crystallinity, leading to obviously enhancement in photocatalytic performance.

The photocatalyst performance also can be visually represented by colour alteration of the MO solution after up to 120 min of the UV light illumination, as shown in Fig. 6. Level of the color discrepancies after irradiation indicates the performance of the photocatalyst. The greater color alteration of the MO solution indicates that the corresponding photocatalyst has a higher performance. In

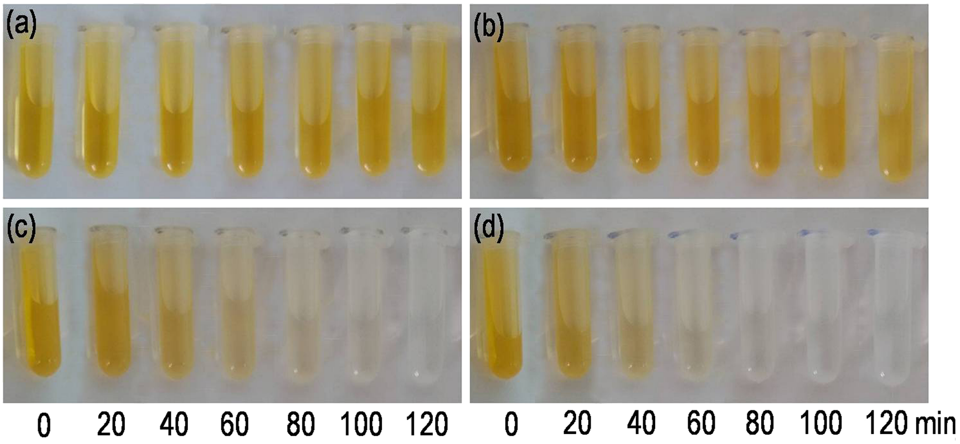

FIG. 6. Colors alteration of MO solution after UV-light irradiation with TiO_2 photocatalyst of (a) 50, (b) 200, (c) 400, and (d) 1000 ALD cycles, calcined at 800 °C.

Fig. 6, the lowest color alteration was observed for MO solution degraded by TiO_2 of 50 ALD cycles. On the contrary, the highest color alteration is the solution degraded with the TiO_2 of 1000 ALD cycles, although the same amount of photocatalyst (and therefore smaller contact area) was used in the experiment. The observation is consistent with the quantitative results demonstrated in Fig. 5.

Furthermore, we compared the photocatalytic performance of our samples to the values reported in the previous works. In the work carried out by Kansal *et al.*,[42] the TiO_2-ZnO composite (TiO_2-ZnO = 1:1) in particle structure with the photocatalyst concentration of 1 g/L, needs 5 h to degrade ~ 70 % lignin solution. In addition, Tian *et al.*[43] have fabricated TiO_2-ZnO particles and found they were able to degrade MO solution up to ~ 73 % with the degradation time of 3 h (photocatalyst concentration of 0.5 g/L).[43] Our samples show excellent performance compared with those results reported in previous literatures, although they use larger photocatalyst concentrations. We preliminarily ascribed the enhancement to the nanomembrane structures with larger surface areas and better crystal quality.

IV. CONCLUSIONS

In this study, TiO_2 and TiO_2-ZnO were well deposited onto the polyurethane porous sponge template by ALD at relatively low temperature. The three-dimensionally semiconductor porous structures which duplicate the structure of original sponge templates were obtained after calcination, which were then broken into small pieces by a manual pulverizing process. Experimental results indicates the thickness of nanomembrane has effect on the degree of crystallinity: the crystallinity is raised by increasing the thickness due to fewer grain boundaries. Correspondingly, the photocatalytic performance is also enhanced in the thicker nanomembrane. Another way to boost the photocatalytic performance is by coupling TiO_2 with ZnO to form composites structure. It shows the photocatalytic performance raises consistently with increasing the ZnO concentration in the TZO composite.

ACKNOWLEDGMENTS

This work was supported by the National Natural Science Foundation of China (Nos. 51322201 and 51475093) and Science and Technology Commission of Shanghai Municipality (Nos. 14JC1400200 and 12PJ1400500).

[1] C. Cheng, A. Amini, C. Zhu, Z. Xu, H. Song, and N. Wang, Sci. Rep. **4**, 1 (2014).
[2] J. Tian, L. Chen, J. Dai, X. Wang, Y. Yin, and P. Wu, Ceram. Int. **35**, 2261 (2009).
[3] M. Pelaez, N. T. Nolan, S. C. Pillai, M. K. Seery, P. Falaras, A. G. Kontos, P. S. M. Dunlop, J. W. J. Hamilton, J. A. Byrne, K. O'Shea, M. H. Entezari, and D.D. Dionysiou, Appl. Catal. B: Environmental **125**, 331 (2012).
[4] K. Nakata and A. Fujishima, J. Photochem. Photobiol. C: Photochem. Rev. **13**, 169 (2012).
[5] K. Maeda and K. Domen, J. Phys. Chem. Lett. **1**, 2655 (2010).
[6] H. Tong, S. Ouyang, Y. Bi, N. Umezawa, and M. Oshikiri, Adv. Mater. **24**, 229 (2012).
[7] R.-H. Tao, J.-M. Wu, J.-Z. Xiao, Y.-P. Zhao, and W.-W. Dong, Appl. Surf. Sci. **279**, 324 (2013).
[8] E. García-Ramírez, M. Mondragón-Chaparro, and O. Zelaya-Angel, Appl. Phys. A – Mater. Sci. Proc. **108**, 291 (2012).
[9] B. Pant, H. R. Pant, N. A. M. Barakat, M. Park, K. Jeon, Y. Choi, and H.-Y. Kim, Ceram. Int. **39**, 7029 (2013).
[10] A. I. Kontos, I. M. Arabatzis, D. S. Tsoukleris, A. G. Kontos, M. C. Bernard, D. E. Petrakis, and P. Falaris, Catal. Today **101**, 275 (2005).
[11] J. Zhang, L. Qian, L. Yang, X. Tao, K. Su, H. Wang, J. Xi, and Z. Ji, Appl. Surf. Sci. **311**, 521 (2014).
[12] P. Roy, S. Berger, and P. Schmuki, Angew. Chem. Int. Ed. **50**, 2904 (2011).
[13] Y. Liao, C. Xie, Y. Liu, H. Chen, H. Li, and J. Wu, Ceram. Int. **38**, 4427 (2012).
[14] G. Marcì, V. Augugliaro, M. J. López-Muñoz, C. Martin, L. Palmisano, V. Rives, M. Schiavello, R. J. D. Tilley, and A. M. Venezia, J. Phys. Chem. B **105**, 1026 (2001).
[15] G. Marcì, V. Augugliaro, M. J. López-Muñoz, C. Martin, L. Palmisano, V. Rives, M. Schiavello, R.J. D. Tilley, and A. M. Venezia, J. Phys. Chem. B **105**, 1033 (2001).
[16] K. Lee, M. D. Losego, D. H. Kim, and G. N. Parsons, Mater. Horizons **1**, 419 (2014).
[17] N. Roy, Y. Sohn, and D. Pradhan, ACS Nano **7**, 2532 (2013).
[18] L. Peng, H. Zhang, Y. Bai, Y. Feng, and Y. Wang, Chem.-A Eur. J. **21**, 14871 (2015).
[19] S. Q. Pan, Y. Zhao, G. S. Huang, J. Wang, S. Baunack, T. Gemming, M. L. Li, L. R. Zheng, O. G. Schmidt, and Y. F. Mei, Nanotechnology **26**, 364001 (2015).
[20] I. Jang, J.-H. Park, K. Song, S. Kim, Y. Lee, and S.-G. Oh, Mater. Chem. Phys. **147**, 691 (2014).
[21] S. Pavasupree, Y. Suzuki, S. Yoshikawa, and R. Kawahata, J. Sol. State Chemistry **178**, 3110 (2005).
[22] K. Eufinger, D. Poelman, H. Poelman, R. D. Gryse, and G. B. Marin, in *Thin Solid Films: Process and Applications*, edited by S. C. Nam, (Transworld Research Network, Kerala, India, 2008), pp. 189–227.
[23] J. Tian, L. Chen, Y. Yin, X. Wang, J. Dai, Z. Zhu, X. Liu, and P. Wu, Surf. Coat. Technol. **204**, 205 (2009).
[24] S. Ji, S. Murakami, M. Kamitakahara, and K. Ioku, Mater. Res. Bull. **44**, 768 (2009).

[25] J. B. Joo, I. Lee, M. Dahl, G. D. Moon, F. Zaera, and Y. Yin, Adv. Func. Mater. **23**, 4246 (2013).
[26] R. Fernandes, N. Patel, R. Dholam, M. Adami, and A. Miotello, Surf. Coat. Technol. **203**, 2579 (2009).
[27] F. Dufour, S. Pigeot-Remy, O. Durupthy, S. Cassaignon, V. Ruaux, S. Torelli, L. Mariey, F. Maugé, and C. Chanéac, Appl. Catal. B: Environmental **174**, 350 (2015).
[28] M. A. Henderson, Surf. Sci. Rep. **66**, 185 (2011).
[29] M. Batzill, Energy Environ. Sci. **4**, 3275 (2011).
[30] R. Marschall, Adv. Func. Mater. **24**, 2421 (2014).
[31] S. Bai, W. Jiang, Z. Li, and Y. Xiong, Chem Nano Mat. **1**, 223 (2015).
[32] R. Edy, Y. T. Zhao, G. S. Huang, J. J. Shi, J. Zhang, A. A. Solovev, and Y. F. Mei, "TiO_2 nanosheets synthesized by atomic layer deposition for photocatalysis," Prog. Nat. Sci.: Mater. Int. (2016) (Accepted).
[33] A. P. Alekhin, S. A. Gudkova, A. M. Markeev, A. S. Mitiaev, A. A. Sigarev, and V. F. Toknova, Appl. Surf. Sci. **257**, 186 (2010).
[34] M. Moret, A. A. Chaaya, M. Bechelany, P. Miele, Y. Robin, and O. Briot, Superlatt. Microstruc. **75**, 477 (2014).
[35] K. Vajda, Z. Kása, A. Dombi, Z. Németh, G. Kovács, V. Danciu, T. Radu, C. Ghica, L. Baia, K. Hernádi, and Z. Pap, Nanoscale **7**, 5776 (2015).
[36] M. A. Johar, R. A. Afzal, A. A. Alazba, and U. Manzoor, Adv. Mater. Sci. Eng. **2015**, 934587 (2015).
[37] M. Gholami, M. Shirzad-Siboni, M. Farzadkia, and J.-K. Yang, Desal. Wat. Treat. **57**, 13632 (2016).
[38] D. Chatterjee and S. Dasgupta, J. Photochem. Photobiol. C: Photochem. Rev. **6**, 186 (2005).
[39] M. Bizarro, Appl. Catal. B: Environmental **97**, 198 (2010).
[40] M. A. Gondal, A. M. Ilyas, and U. Baig, Ceram. Int. **42**, 13151 (2016).
[41] C. C. Pei and W. W.-F. Leung, Separ. Pur. Technol. **114**, 108 (2013).
[42] S. K. Kansal, M. Singh, and D. Sud, J. Hazard. Mater. **153**, 412 (2008).
[43] J. Tian, J. Wang, J. Dai, X. Wang, and Y. Yin, Surf. Coat. Technol. **204**, 723 (2009).
[44] T. Tynell and M. Karppinen, Semicond. Sci. Technol. **29**, 043001 (2014).
[45] M. Godlewski, E. Guziewicz, G. Luka, T. Krajewski, M. Lukasiewicz, L. Wachnicki, A. Wachnicka, K. Kopalko, A. Sarem, and B. Dalati, Thin Solid Films **518**, 1145 (2009).
[46] A. Shafaei, M. Nikazar, and M. Arami, Desalination **252**, 8 (2010).
[47] U. I. Gaya and A. H. Abdullah, J. Photochem. Photobiol. C: Photochem. Rev. **9**, 1 (2008).
[48] M. L. Li, G. S. Huang, Y. Qiao, J. Wang, Z. Liu, X. Liu, and Y. F. Mei, Nanotechnology **24**, 305706 (2013).